Visible-light-induced activation of periodate that mimics dye-sensitization of TiO_2: Simultaneous decolorization of dyes and production of oxidizing radicals

Eun-Tae Yun [a,1], Ha-Young Yoo [b,c,1], Wooyul Kim [d,1], Hyung-Eun Kim [e], Gyeongho Kang [f], Hongshin Lee [e], Seunghak Lee [b,c], Taiho Park [f], Changha Lee [e], Jae-Hong Kim [g], Jaesang Lee [a,b,*]

[a] Civil, Environmental, and Architectural Engineering, Korea University, Seoul 136-701, Republic of Korea
[b] Energy Environmental Policy and Technology, Green School, Korea University-KIST, Seoul 136-701, Republic of Korea
[c] Center for Water Resource Cycle Research, Korea Institute of Science and Technology, Seoul 136-791, Republic of Korea
[d] Chemical and Biological Engineering, Sookmyung Women's University, Seoul, 04310, Republic of Korea
[e] Urban and Environmental Engineering, KIST-UNIST-Ulsan Center for Convergent Materials (KUUC), Ulsan National Institute of Science and Technology, Ulsan 698-805, Republic of Korea
[f] Chemical Engineering, Polymer Research Institute, Pohang University of Science and Technology, Pohang 790-784, Republic of Korea
[g] Chemical and Environmental Engineering, Yale University, New Haven, CT 06511, United States
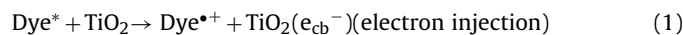
ARTICLE INFO

ABSTRACT

Inspired by the mechanism behind self-sensitized destruction of dyes on semiconductor photocatalysts, we herein present the first instance of visible-light-induced activation of periodate (IO_4^-) into reactive iodine radicals via sensitized electron transfer from an organic dye, Rhodamine B (RhB). The IO_4^- reduction not only leads to oxidative decolorization of RhB but also formation of reactive intermediates that degrade organic compounds. Electron transfer from the excited dye to IO_4^- was confirmed by detecting RhB radical cation ($RhB^{\bullet+}$) and measuring its lifetime. The efficiency of organic compound degradation was found to significantly vary depending on the target substrate, i.e., phenol, bisphenol A, and 4-chlorophenol were rapidly decomposed, whereas benzoic acid, carbamazepine, 4-nitrophenol, and sulfamethoxazole exhibited moderate decomposition rate. Lines of evidence in addition to the substrate specificity, such as insignificant hydroxylation, non-stoichiometric dechlorination, and marginal quenching effects of organic/inorganic compounds (e.g., methanol, natural organic matters, and chloride ion), points toward the involvement of iodate radical ($IO_3^\bullet$). The dye-sensitized IO_4^- activation process was also found to be highly effective in inactivation of MS2 bacteriophage.

© 2016 Elsevier B.V. All rights reserved.

1. Introduction

A dye molecule that forms its excited triplet-state through visible light absorption and subsequent intersystem crossing can transfer its absorbed energy to ground triplet-state oxygen [1,2]. This energy transfer process results in photosensitized production of singlet oxygen ($^1O_2$), an oxidant that is known to degrade organic pollutants and inactivate bacteria and viruses [3,4]. Alternatively, the excited triplet-sta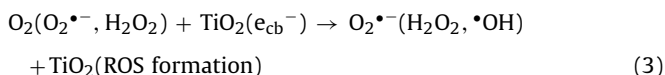te of dye can transfer its electron to an electron acceptor, which leads to the oxidation of dye and generation of reactive oxygen species (ROS) [5,6]. Such an electron transfer is fundamental to various dye-sensitized processes such as dye-sensitized solar cells [7] and dye-sensitized photocatalysis [5,6]. For example, reactions presented below account for how visible-light-driven photocatalysis is achieved with large bandgap semiconductors such as TiO_2 [8,9]. The dye forms radical cation ($dye^{\bullet+}$) (Reaction 1) and further reacts with oxygen to form oxidized products (Reaction 2), while superoxide radical anion ($O_2^{\bullet-}$) reductively converts into H_2O_2 and hydroxyl radical ($^\bullet OH$) (Reaction 3) [5,6]. Note that electron transfer mediator, TiO_2 in this mechanism, is essential, since direct electron transfer from the excited dyes and oxygen is in general not kinetically favored [9].

$$Dye^* + TiO_2 \rightarrow Dye^{\bullet+} + TiO_2(e_{cb}^-)(\text{electron injection}) \quad (1)$$

$$\text{Dye}^{\bullet+} + O_2 \rightarrow \rightarrow \text{oxidized products (further oxidation)} \qquad (2)$$

$$O_2(O_2^{\bullet-}, H_2O_2) + TiO_2(e_{cb}^-) \rightarrow O_2^{\bullet-}(H_2O_2, {}^{\bullet}OH)$$
$$+ TiO_2(\text{ROS formation}) \qquad (3)$$

A similar electron transfer scheme might be possible by employing an alternative electron acceptor such as periodate (IO_4^-). For example, an oxyanion such as IO_4^- is known to effectively accept electron from photosensitized WO_3, even outcompeting oxygen [10]. It is interesting to note that such a reaction appears to be dependent on the type of electron acceptor, since other inorganic oxyanions such as H_2O_2, peroxymonosulfate (HSO_5^-), peroxydisulfate ($S_2O_8^{2-}$) do not function efficiently [10]. This leads us to postulate that electrons from the excited dyes can be also transferred to IO_4^-. If such a process were kinetically favored, it might not even require the electron transfer mediator such as TiO_2 or WO_3. We recognize that the activation of IO_4^- via iron-based bimetallic nanoparticles (e.g., nFe^0-Ni) [11] and UV photolysis [12,13] can lead to the formation of reactive radical intermediates (e.g., ${}^{\bullet}OH$ and/or iodate radical ($IO_3^{\bullet}$)). Consequently, potential dual roles by IO_4^- are hypothesized; i.e., accepting electron from photosensitized dye and producing reactive radicals.

This study reports IO_4^- activation through dye-sensitization (*mimicking self-sensitized dye decolorization on TiO_2* [14]) for the first time in literature. We employ select organic dyes such as Rhodamine B (RhB) and Methylene Blue (MB) and tested whether the postulated electron transfer to IO_4^- and other select electron acceptors such as HSO_5^-, $S_2O_8^{2-}$, and H_2O_2 occurs when visible light ($\lambda > 400$ nm) is irradiated. In addition to the anticipated dye oxidation, we further tested whether select organic compounds such as phenol, benzoic acid, bisphenol A, carbamazepine, 4-chlorophenol, 4-nitrophenol, and sulfamethoxazole can be also degraded due to the reaction with reactive radicals that form via IO_4^- activation. Our study is focused on elucidating the fundamental reaction pathways through kinetics evaluation, transient absorption spectral analysis, and laser flash photolysis, but also addresses the effect of engineering parameters such as initial concentration of RhB, IO_4^- dosage, and initial pH as well as the potential for inactivation of *Escherichia coli* (*E. coli*) and MS2 bacteriophage (MS2 phage).

2. Materials and methods

2.1. Reagents

The following chemicals were used as received: Crystal Violet (CV, Sigma), Methylene Blue (Sigma-Aldrich), Methyl Orange (MO, Sigma-Aldrich), Reactive Black 5 (RB5, Sigma–Aldrich), Rhodamine B (Sigma), benzoic acid (Sigma–Aldrich), bisphenol A (Aldrich), carbamazepine (Sigma–Aldrich), 4-chlorophenol (Aldrich), 4-nitrophenol (Aldrich), phenol (Sigma–Aldrich), sulfamethoxazole (Fluka), hydrogen peroxide solution (30 wt% in H_2O, Sigma–Aldrich), sodium periodate (Sigma–Aldrich), OXONE® monopersulfate compound (PMS, Sigma-Aldrich), potassium peroxodisulfate (PDS, Sigma–Aldrich), methanol (Sigma–Aldrich), perchloric acid (Sigma–Aldrich), sodium hydroxide (Fluka), phosphoric acid (Aldrich), and acetonitrile (J.T. Baker). Agar, nutrient broth, tryptone, and yeast extract were obtained from Becton Dickinson. Ultrapure deionized water (>18 MΩ cm), produced with a Millipore system, was used for the preparation of all experimental solutions. All chemicals were of reagent grade and were used without further purification or treatment.

2.2. Photochemical experiments

Photosensitization reactions were performed in a magnetically stirred cylindrical quartz reactor at ambient temperature (22 °C) under irradiation by a 150 W Xe-arc lamp (Abet Technologies, LS-150) through a UV cut-off filter ($\lambda > 400$ nm). Photochemical activation of IO_4^- under UVA illumination was carried out with six 4-W black-light blue lamps (Philips Co.). The incident light intensity of the Xe-arc lamp and the black light blue lamp was measured using a power meter (Newport 1918-R) with a silicon diode detector and was determined to be 260.3 mW/cm^2 and 2.26 mW/cm^2, respectively. Fig. S1 shows the emission spectra of the applied light sources (recorded using a Spectropro-500 spectrophotometer (Acton Research Co.) and a spectroradiometer (Luzchem SPR-4001)). Select experiments were performed using a solar simulator (Peccell Technologies, Inc, PEC-L01) as a light source.

The photosensitization reaction solutions comprised 50 μM photosensitizer (e.g., RhB), 50 μM organic target substrate (e.g., phenol), and 0.5 mM IO_4^- as an electron acceptor. The pH of the solution was initially adjusted to 7.0 with 1 M $HClO_4$ or NaOH and changed negligibly during the course of the photosensitization reaction. The experimental solution was un-buffered and air-equilibrated. During progress of the photochemical reaction, 1 mL aliquots of the reaction mixture were periodically withdrawn from the reactor at a predetermined interval using an 1-mL syringe, filtered through a 0.45 μm PTFE filter (Millipore), and transferred to a 2-mL amber glass vial. Experiments were carried out in at least duplicate for each experimental condition. The residual concentrations and time-dependent change in the absorption spectra of the photosensitizing dyes were monitored using a UV–vis spectrophotometer (S-3100; Sinco Co.). Quantification of all the organic substrates as well as IO_4^- and IO_3^- was performed by using an HPLC (Shimadzu LC-20AD) equipped with a C-18 column (ZORBAX Eclipse XDB-C18) and a UV/Vis detector (SPD-20AV). The mobile phase comprised a binary mixture of 0.1% (v/v) aqueous phosphoric acid solution and acetonitrile (typically 60:40 by volume).

Time-resolved photoluminescence (TRPL) spectroscopy via time-correlated single photon counting (TCSPC) system (HAMAMATSU/C11367-31) was used to monitor the photoluminescence (PL) decay of excited dye in the nanosecond regime in the absence and presence of IO_4^-. The excitation of select dyes (RhB at 470 nm; MB at 630 nm; MO at 280 nm) was conducted using a light-emitting diode (LED) to produce full-width at half-maximum (FWHM) (<1.0 ns) pulses at a repetition rate of 5 MHz. The PL emission was measured at 580 nm, 690 nm, and 460 nm for RhB, MB, and MO, respectively. The PL lifetimes were determined by fitting mono-exponential decay curves to the empirical data.

2.3. Laser flash photolysis

The laser flash photolysis experiments were carried out to detect RhB radical cation (RhB$^{\bullet+}$) and trace the decay kinetics. A 553 nm laser pulse (10 mJ/pluse, 10 Hz) from an OPO laser system (Continuum, Surelite OPO) pumped by an Nd^{3+}:YAG laser (Continuum, Surelite II-10, 8 ns full width at half-maximum) was used as an excitation source. The excitation was operated with temporal control by a delay generator (Stanford Research Systems, DG535). The transmitted probe light was directed through a monochromator (Nikon G250) to a silicon avalanche photodiode detector (Hamamatsu Photonics, S5343). The transient signals were recorded by a digitizer (Tektronix, TDS 580D). Time-resolved absorption spectra in the wavelength region from 350 to 650 nm were measured using a multichannel analyzer system (Hamamatsu Photonics, C5967). Instantaneous formation of RhB$^{\bullet+}$ after laser pulse and subsequent

decay were monitored by recording the transient absorption at 490 nm.

2.4. Photosensitized bacterial and viral inactivation

The photosensitizing bactericidal and virucidal activity was evaluated using *E. coli* (ATCC 8739) and MS2 bacteriophage (ATCC 15597-B1). *E. coli* was cultured with 30 mL of 8 g/L nutrient broth for 18–24 h at 37 °C. The cells were harvested by centrifugation at $3000 \times g$ for 15 min and subsequently washed three times with phosphate-buffered saline (PBS, pH 7.2). The *E. coli* stock was prepared by resuspending the collected cells in 20 mL PBS and stored at 4–5 °C. The final concentration was determined by a spread plate method on nutrient agar after 18–24 h incubation at 37 °C [15]. The MS2 phage was prepared using *E. coli* strain C3000 (ATCC 15597) as the host. The C3000 strain was cultivated with 30 mL of broth containing 1% tryptone, 0.8% NaCl, 0.1% yeast extract, 0.01% glucose, 2 mM $CaCl_2$, and 0.001% thiamine. After inoculation of *E. coli* C3000 with MS2 phage and subsequent overnight incubation, the culture solution was subjected to centrifugation, and the supernatant was filtered through a 0.22-μm nylon filter. MS2 phage quantification was conducted by the soft agar overlay (double-agar layer) plaque assay method [15]. Photosensitized disinfection was performed using the Xe-arc lamp with a UV cut-off filter ($\lambda > 400$ nm). The experimental solution (10 mM phosphate buffer at pH 7.0) contained 50 μM RhB, 0.1–0.5 mM IO_4^-, and either *E. coli* at 10^7 colony forming units (CFU)/mL or MS2 phage at 10^7 plaque forming units (PFU)/mL. Then, 1 mL samples were withdrawn at fixed time intervals for quantifying the viable *E. coli* or MS2 phages. The inactivation experiments were repeated at least in triplicate.

3. Results and discussion

3.1. RhB and phenol degradation in the presence of IO_4^-

RhB was found to be rapidly decolorized by IO_4^- under visible light irradiation (Fig. 1a). The RhB oxidation was accompanied by stoichiometric reduction of IO_4^- to IO_3^-. However, we did not observe significant reaction in the dark (RhB degradation efficiency did not exceed *ca.* 6%). (Fig. 1a; RhB/IO_4^-). In addition, RhB alone was not degraded by visible light irradiation in the absence of IO_4^- (Fig. 1a; RhB/Vis). Likewise, IO_4^- alone did not transform to IO_3^- in the absence of RhB under visible light irradiation (Fig. 1a; IO_4^-/Vis). These results, along with the finding that no iodinated products formed, suggest that facile electron transfer from photo-excited RhB (RhB*) to IO_4^- results in RhB oxidation and IO_4^- reduction.

By adding phenol to the above RhB/IO_4^- system under visible-light irradiation, we observed a very rapid degradation of phenol (Fig. 1b). We also found that the kinetics of RhB degradation, IO_4^- reduction, and IO_3^- formation were similar to those we had previously observed in the absence of phenol. Control experimental results in which RhB or IO_4^- alone did not lead to phenol degradation (Fig. 1b) rule out the possibility that phenol oxidation resulted from RhB photosensitization (which could form $^1O_2$) or IO_4^- activation by visible light [2,12,13]. Instead, phenol oxidation is likely to occur due to synchronous IO_4^- reduction to IO_3^- and photosensitized oxidation of RhB. If IO_4^- were reduced to IO_3^- through an unlikely two-electron transfer from RhB, phenol oxidation should not have followed. Therefore, additional electron acceptor is likely involved in phenol degradation, such as $IO_3^\bullet$ that forms through one-electron reduction of IO_4^- [11], or possibly other radicals such as $^\bullet OH$ formed through UV-induced IO_4^- activation [12,13]. The stoichiometric release of IO_3^- (Fig. 1b) reconfirms no occurrence of iodinated organic intermediates that may form via phenol oxidation in the RhB/IO_4^- system. Neither IO_3^- nor phenol decomposed

at all under visible light irradiation when IO_3^- was alternative used in the ternary system (i.e., RhB/phenol/IO_3^-) (Fig. S2), which implies no further reduction of IO_3^- to I^-. The observation that phenol decomposition was significantly faster than RhB decolorization (Fig. 1b) also suggests the possible involvement of the additional, fast reaction pathway (involving catalytic regeneration of RhB).

3.2. Alternative electron acceptors and sensitizers

For the electron transfer scheme postulated above, IO_4^- was found to be a uniquely efficient electron acceptor (Fig. 2a). Other benchmark oxyanions such as HSO_5^-, $S_2O_8^{2-}$, and H_2O_2 did not cause RhB degradation under the same visible light irradiation, despite relatively high reduction potential ($E^0(S_2O_8^{2-}/SO_4^{2-}) = 1.96$ V [16]; $E^0(HSO_5^-/HSO_4^-) = 1.82$ V [17]; $E^0(H_2O_2/H_2O) = 1.776$ V [16]), which is higher than IO_4^- ($E^0(IO_4^-/IO_3^-) = 1.298$ V [18]). This implies that the electron transfer from RhB* to IO_4^- may be kinetically preferred. The superiority of IO_4^- over other inorganic oxidants in photosensitized decolorization is consistent with the earlier observation [10] that IO_4^- functioned as an effective electron acceptor, remarkably improving the photocatalytic activity of WO_3 for 4-chlorophenol degradation, whereas HSO_5^-, $S_2O_8^{2-}$, and H_2O_2 were ineffective. The RhB decolorization that appeared pronounced in the presence of IO_4^- (Fig. 2a) may be related to the preferential interaction between RhB and IO_4^-. However, the comparison of the UV–vis absorption spectra of RhB alone and RhB in combination with oxyanions (i.e., IO_4^-, HSO_5^-, and $S_2O_8^{2-}$) indicated no distinction in spectral features (Fig. S3), which likely rules out the possibility of the formation of a charge transfer complex consisting of RhB and IO_4^-.

We further examined whether other dye sensitizers (absorption spectra and chemical structures provided in Figs. S1 and S4) could also initiate the similar redox scheme in the presence IO_4^- under visible light irradiation (Fig. 2b). These dyes were not degraded by neither visible light irradiation alone (Fig. S5) nor IO_4^- alone in the dark (Fig. S6). We observed significant decolorization of MB at the rate very similar to that of RhB (Fig. 2b). Degradation of CV occurred at a moderate rate and RB5 at even slower rate, while MO was not degraded at all. Time-dependent changes in the UV–vis absorption spectra of these dyes are presented in Fig. S7. The dye-specific degradation kinetics observed in Fig. 2b are in marked contrast to those in UV-activated IO_4^- system in which the kinetics were relatively constant regardless of dye type (Fig. S8). This clear distinction implies that the dye/IO_4^-/Vis system induced the main oxidation mechanism entirely different from the IO_4^-/UV system. Note that the UV-activated IO_4^- is known to produce non-selective and highly reactive $^\bullet OH$ according to the intramolecular electron transfer mechanism (i.e., $IO_4^- + h\nu \rightarrow IO_3^\bullet + O^{\bullet-}$; $O^{\bullet-} + H+ \leftrightarrow {}^\bullet OH$) [12,13]. Similar to dyes, phenol degradation kinetics also depended on the type of dye (Fig. 2b; inset), strengthening the notion that $^\bullet OH$ is not involved. If visible light dissociated IO_4^- to generate $^\bullet OH$ as a main oxidant in some way, the rate of phenol oxidation by the dye/IO_4^- mixture would not vary significantly according to the type of dye. We can also exclude the possibility that phenol oxidation occurred due to singlet oxygen generated from the photo-excited dyes, since visible light irradiation of dyes in the absence of IO_4^- did not lead to phenol degradation (Fig. S9) [2]. These results are consistent with the aforementioned postulation that dye degradation is most likely related to direct electron transfer from photosensitized dye to IO_4^- and the accompanying phenol degradation to the formation of an intermediate oxidant other than $^\bullet OH$.

3.3. Electron transfer from RhB to IO_4^-

First, we tested the hypothesis that electrons transfer from photosensitized dye to IO_4^- using the time-resolved PL (Fig. 3). The
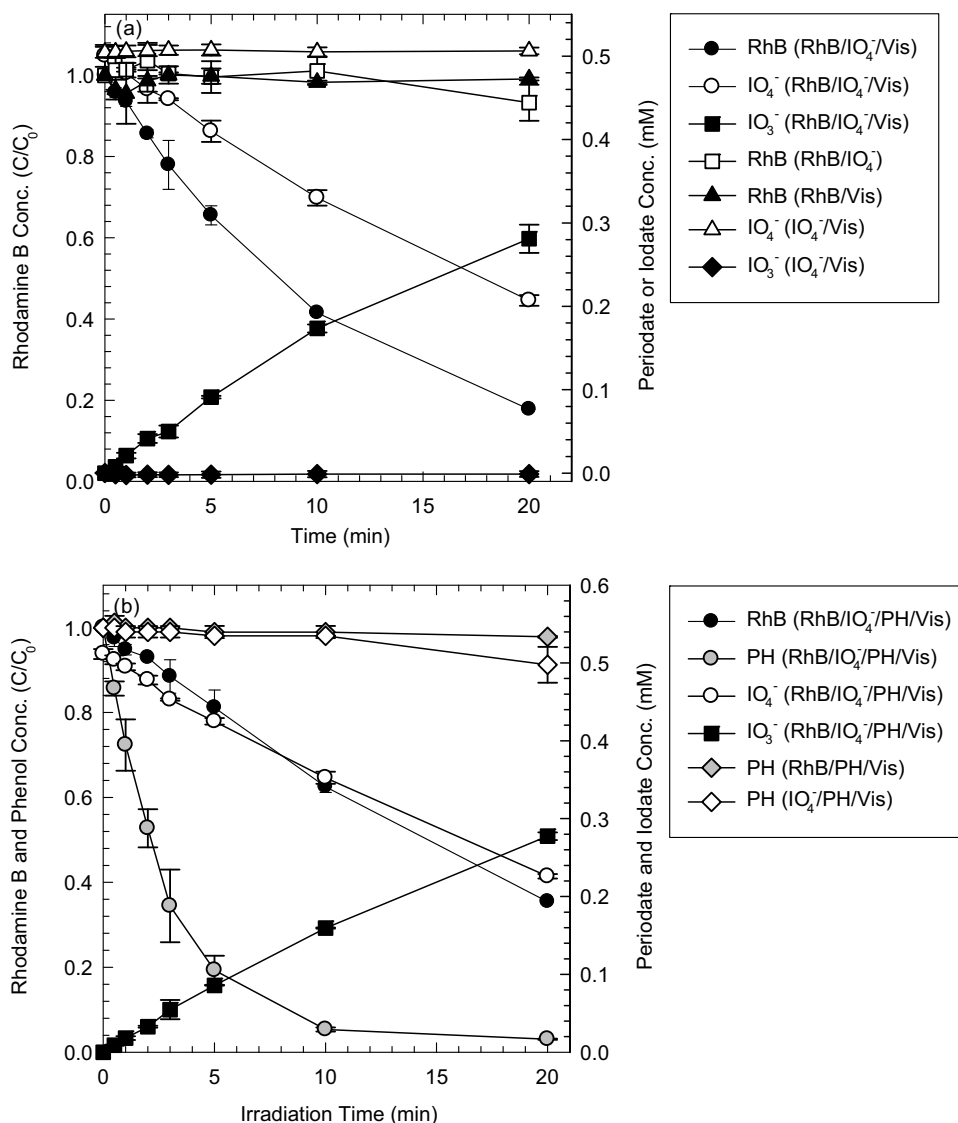
Fig. 1. (a) Self-sensitized destruction of Rhodamine B in the presence of periodate (i.e., RhB/IO$_4^-$) under visible light irradiation and (b) concurrent decolorization of Rhodamine B, degradation of phenol, and reduction of periodate into iodate in visible-light-illuminated aqueous ternary system (i.e., RhB/PH/IO$_4^-$) ([Rhodamine B]$_0$ = [phenol]$_0$ = 50 μM; [periodate]$_0$ = 0.5 mM; pH$_i$ = 7.0).

decay of RhB* was significantly accelerated due to IO$_4^-$, from τ(PL lifetime of RhB) = 1.78 ns (without IO$_4^-$) versus τ(RhB) = 0.96 ns (with IO$_4^-$). Decay kinetics of excited-state MB (MB*) was accelerated modestly, from τ(MB) = 370 ps (without IO$_4^-$) to τ(MB) = 290 ps (with IO$_4^-$) (Fig. S10), while that of excited-state MO (MO*) did not change (i.e., τ(MO) = 2.37 ns (without IO$_4^-$) versus τ(MO) = 2.38 ns (with IO$_4^-$)). This trend is consistent with the dependency of dye and phenol degradation on the type of dye (Fig. 2b). The efficiency of the intermolecular electron transfer from excited-state dye to IO$_4^-$ is determined by various factors such as quantum efficiency of the photo-excitation, energy level of the excited state, and ionic charge (and consequently the electrostatic interaction between dye and IO$_4^-$). For instance, the preferential electron transfer of cationic dyes (e.g., RhB, MB) to IO$_4^-$ and their rapid decolorization (Fig. 2b) appear partially relevant to the attractive interaction with IO$_4^-$. On the other hand, self-sensitized dye decolorization and reductive conversion of IO$_4^-$ to reactive iodine intermediates (indirectly indicated by phenol decomposition) negligibly occurred (Fig. 2b) when anionic dyes (e.g., MO) that interact repulsively with IO$_4^-$ were alternatively used. While elucidating such variations (especially related to intrinsic photophysical and photochemical properties of dyes) is not the focus of this study, this result provides convincing evidence for electron transfer from excited dye to IO$_4^-$.

Formation of RhB$^{\bullet+}$ is the direct consequence of electron transfer from RhB* to IO$_4^-$; we therefore probed RhB$^{\bullet+}$ formation through the laser flash photolysis with 533-nm pulse excitation of RhB. Following the excitation, transient absorption spectra showed the emergence of transient absorbance at 490 nm (RhB$^{\bullet+}$) [19] and 553 nm (RhB) (Fig. 4a, spectrum obtained 100 μs after the laser flash photolysis). Results suggest instant formation of RhB$^{\bullet+}$ and subsequent decay of RhB$^{\bullet+}$ over millisecond duration (Fig. 4a; inset). The absorption peak (490 nm) assigned to RhB$^{\bullet+}$ was not observed in the absence of IO$_4^-$ (Fig. S11), which suggests that RhB* can not directly reduce O$_2$ (to O$_2^{\bullet-}$) and IO$_4^-$ (electron acceptor) is required to oxidize RhB (electron donor) and to form RhB$^{\bullet+}$. Consistently, as initial concentration of IO$_4^-$ and laser power were increased, a greater amount of RhB$^{\bullet+}$ formed, hence RhB$^{\bullet+}$ lasted over a longer period (Fig. S12). Also consistent with the observation made in Fig. 2a, RhB$^{\bullet+}$ was not detected when S$_2$O$_8^{2-}$ was used instead of IO$_4^-$ as an electron acceptor (Fig. 4a).
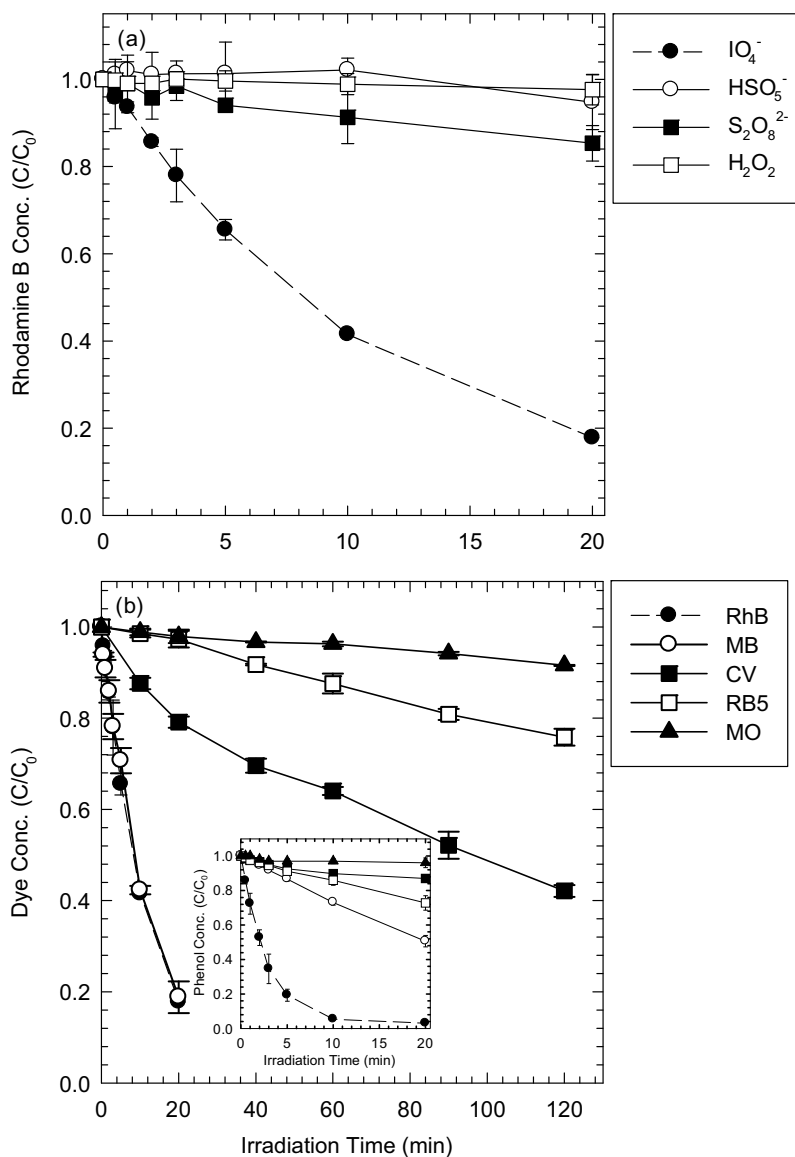
Fig. 2. (a) Rhodamine B decoloration in the visible-light-illuminated aqueous solutions of various inorganic oxyanions ([Rhodamine B]$_0$ = 50 μM; [periodate]$_0$ = [peroxymonosulfate]$_0$ = [peroxydisulfate]$_0$ = [hydrogen peroxide]$_0$ = 0.5 mM; pH$_i$ = 7.0) and (b) Self-sensitized decolorization of dyes in the presence of periodate under visible light irradiation (inset: phenol degradation by the dye/IO$_4^-$ systems) ([dye]$_0$ = [phenol]$_0$ = 50 μM; [periodate]$_0$ = 0.5 mM; pH$_i$ = 7.0).

3.4. Oxidative degradation of organics

Second, we further elaborated on the substrate specificity of the RhB/IO$_4^-$ system under visible light irradiation to obtain further insights on the identity of the oxidant responsible for phenol degradation. Results shown in Fig. 5 suggest that the degradation kinetics varied significantly depending on the organic compounds. Decomposition of bisphenol A (k = 0.1843 ± 0.0169 min^{-1}) and 4-chlorophenol (k = 0.2233 ± 0.0124 min^{-1}) proceeded rapidly in the mixture of RhB/IO$_4^-$ under visible light irradiation at a rate comparable to that of phenol, whereas benzoic acid (k = 0.0836 ± 0.0035 min^{-1}) and sulfamethoxazole (k = 0.0593 ± 0.0016 min^{-1}) were degraded at moderate rates. In contrast, 4-nitrophenol (k = 0.0376 ± 0.0007 min^{-1}) and carbamazepine (k = 0.031 ± 0.0080 min^{-1}) were degraded at much slower rate. It is interesting to note that this tendency is remarkably similar to that in IO$_4^-$ activated with UV photolysis when excess methanol is added as an •OH scavenger or that in IO$_4^-$ activated using bimetallic iron [11]. Organic compounds that were highly

vulnerable to oxidation by the RhB/IO$_4^-$ system (e.g., bisphenol A and 4-chlorophenol) underwent rapid decomposition by IO$_4^-$ in combination with UV or iron bimetals (e.g., nFe^0-Ni), whereas three IO$_4^-$ activation processes similarly caused slow removal of 4-nitrophenol and carbamazepine [11]. This result not only excludes non-selective •OH as a major oxidant, but also hints that IO$_3$• is likely involved in the degradation of organic compounds, since IO$_3$• has been suggested as a major oxidant in IO$_4^-$/UV (with •OH scavenging) and IO$_4^-$/bimetallic systems [11]. Consistently, the presence of organic or inorganic background constituents such as natural organic matter (NOM), chloride, and phosphate did not affect the kinetics of phenol degradation (Fig. S13).

In addition to the substrate-specific nature, we present the following lines of evidence to exclude the formation of •OH through the alternative electron-transfer route (IO$_4^-$ + H$_2$O + e$^-$ (from RhB*) → IO$_3^-$ + •OH + OH$^-$). First, complete degradation of 4-chlorophenol did not result in the stoichiometric release of chloride ions (Fig. S14), and hydroxylation of benzoic acid to form 4-hydroxybenzoic acid occurred marginally (Fig. S15). Both are
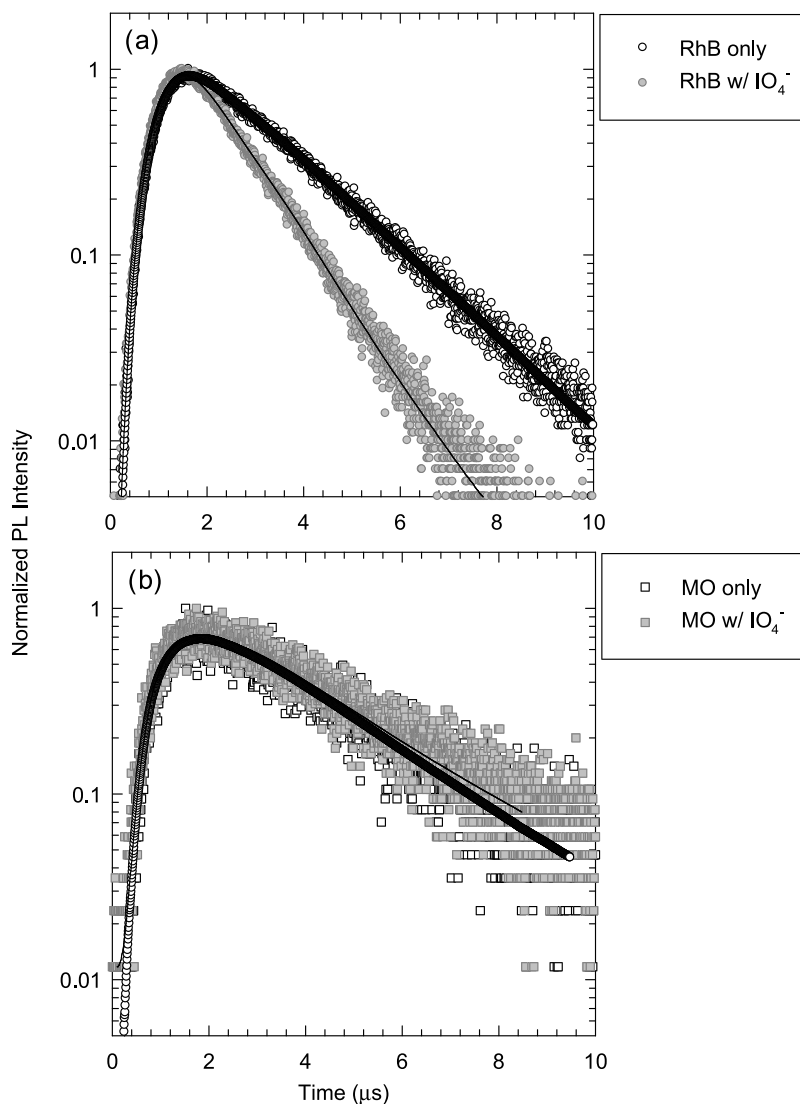
Fig. 3. Photoluminescence (PL) decay of (a) Rhodamine B and (b) Methyl Orange in the absence and presence of periodate ([Rhodamine B]$_0$ = [Methyl Orange]$_0$ = 50 μM; [periodate]$_0$ = 0.5 mM; pH$_i$ = 7.0).

well-known consequence of reactions involving $^\bullet$OH [10,20]. It is noteworthy that chloride ions were stoichiometrically evolved during photocatalytic oxidation of 4-chlorophenol by UV/TiO$_2$ (as an effective producer of $^\bullet$OH) (Fig. S16). Second, no reduction of total organic carbon (TOC) was observed, while phenol was significantly degraded in the RhB/IO$_4^-$ system (Fig. S17). Finally, the presence of 0.1 M methanol as a quencher of $^\bullet$OH did not lead to drastically-decreased efficiency for phenol decomposition (Fig. S13a). In contrast, phenol oxidation by UV/TiO$_2$ was completely quenched on addition of 0.1 M methanol (Fig. S18).

Alternatively, even a relatively low concentration (0.1 mM) of benzoquinone (BQ) completely quenched phenol oxidation (Fig. S13a), which is due to the effective electron accepting capacity of BQ that prevents transfer of electrons from RhB* to IO$_4^-$. The complete quenching effect due to BQ addition is not attributable to free radical scavenging activity of BQ toward reactive oxygen species such as O$_2^{\bullet-}$ [21]. There is very little likelihood that O$_2^{\bullet-}$ could form via electron transfer from RhB* to O$_2$ (i.e., RhB* + O$_2$ → RhB$^{\bullet+}$ + O$_2^{\bullet-}$); we found that RhB$^{\bullet+}$ was not detected after the laser flash photolysis of aqueous RhB solution (Fig. S11) and RhB could not photosensitize phenol oxidation at all without addition of IO$_4^-$ (Fig. 1b). Furthermore, we found that BQ at a concentration

of 0.1 mM did not show drastic retarding effect during the photocatalytic oxidation of phenol by TiO$_2$ where OH and O$_2^{\bullet-}$ serve as oxidizing species (Fig. S18). This result reveals that the radical scavenging activity of 0.1 mM BQ is not sufficient to explain the complete quenching of phenol decomposition by the RhB/IO$_4^-$ system (Fig. S13a).

3.5. Reaction mechanisms

The results presented so far point toward the possible dual roles of IO$_4^-$ in the three-component photosensitizing system that consists of RhB, IO$_4^-$ and phenol (or other organic compounds) under visible light irradiation. First, IO$_4^-$ effectively accepts electron from RhB*, causing oxidative transformation of RhB* to RhB$^{\bullet+}$ (Reaction 4) which shall react with oxygen for further oxidative degradation. Second, IO$_4^-$ is subsequently reduced to IO$_3^\bullet$, which is capable of effectively oxidizing phenol (Reaction (5)). The observation that UV photolysis of IO$_4^-$ (as a source of IO$_3^\bullet$) led to rapid decomposition of all tested dyes (Fig. S8) reveals that oxidation by IO$_3^\bullet$ could be partially responsible for RhB decolorization in the photosensitization system of RhB/IO$_4^-$ (Reaction (5)). Note that various aromatic compounds including select dyes could undergo rapid photosen-
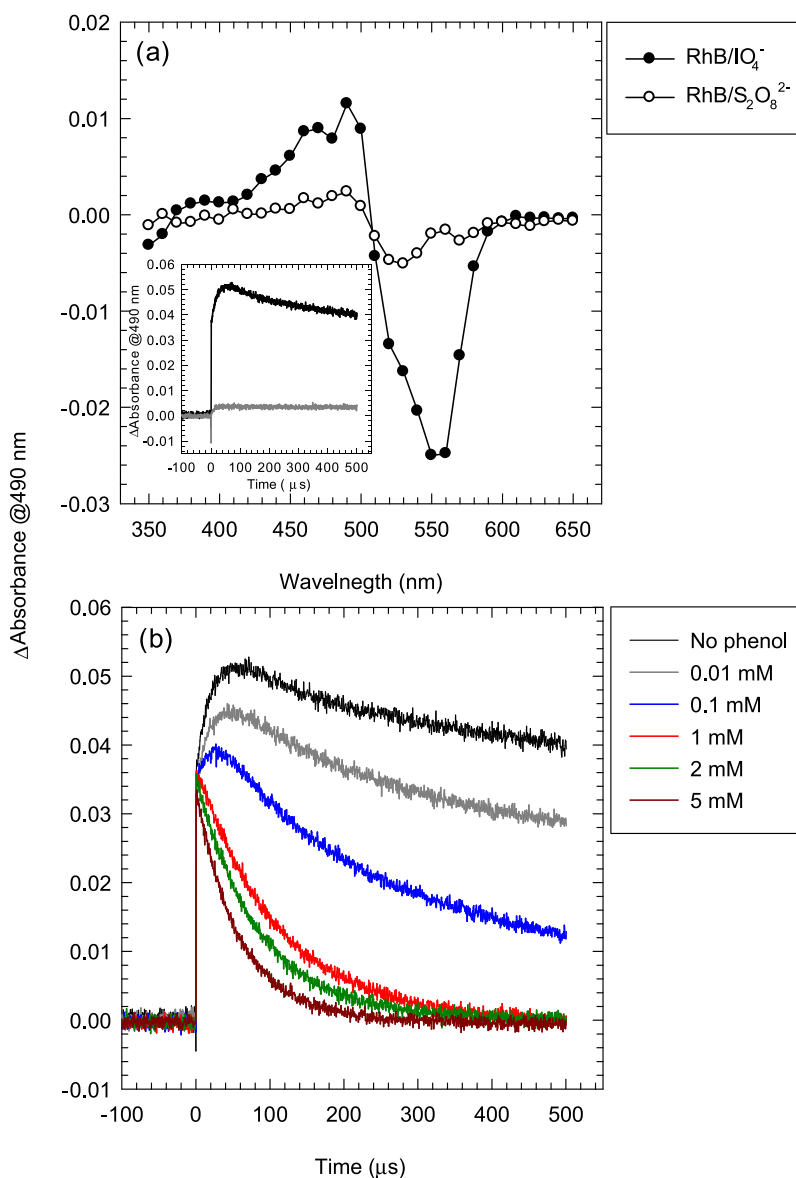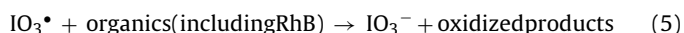
Fig. 4. (a) The transient absorption spectra observed at 100 μs after the laser flash photolysis (at 553 nm) of RhB/IO$_4^-$ and RhB/S$_2$O$_8^{2-}$. Inset: time traces observed at 490 nm. (b) Time traces observed at 490 nm after the laser flash photolysis (at 553 nm) of RhB/IO$_4^-$ with various phenol concentrations ([Rhodamine B]$_0$ = 500 μM; [periodate]$_0$ = [peroxydisulfate]$_0$ = 5 mM; pH$_i$ = 7.0).

sitized decomposition by RhB/IO$_4^-$ (see Fig. 5). This mechanism is illustrated in Scheme 1.

$$RhB^* + IO_4^- \rightarrow RhB^{\bullet+} + IO_3^\bullet \tag{4}$$

$$IO_3^\bullet + organics(includingRhB) \rightarrow IO_3^- + oxidizedproducts \tag{5}$$

With the production of reactive species such as RhB$^{\bullet+}$ and IO$_3^\bullet$, other auxiliary reactions are bound to occur (see Scheme 1). For example, it is possible that relatively long-lived RhB$^{\bullet+}$ reacts with phenol to result in phenol oxidation and concurrent regeneration of RhB (Reaction (6)).

$$RhB^{\bullet+} + organics \rightarrow RhB + oxidizedproducts \tag{6}$$
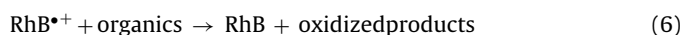
By increasing phenol concentration, we indeed observed that RhB$^{\bullet+}$ decayed much faster (Fig. 4b). With phenol at concentrations exceeding 1 mM, RhB$^{\bullet+}$ was completely depleted within 400 μs, while further increase in phenol concentration did not further accelerate RhB$^{\bullet+}$ decay. The possible role of RhB$^{\bullet+}$ on phenol oxidation may be also responsible for the following observations. First,

oxidative degradation of phenol proceeded at a much faster rate than RhB decolorization (k(phenol) = 0.3243 ± 0.021 min^{-1} versus k(RhB) = 0.0507 ± 0.0014 min^{-1} in Fig. 1b). Note that electron transfer from phenol to RhB$^{\bullet+}$ would contribute to both slower RhB degradation (through RhB regeneration from RhB$^{\bullet+}$) and phenol oxidation. Second, when phenol was added, we also noted that RhB degradation kinetics became slower (k = 0.0864 ± 0.0008 min^{-1} for the RhB/IO$_4^-$ system in Fig. 1a and k = 0.0507 ± 0.0014 min^{-1} for the RhB/phenol/IO$_4^-$ system in Fig. 1b) due to the same reason. Fig. S19 clearly showed that RhB decomposition was gradually decelerated with increasing concentration of phenol, which further corroborates one-electron oxidation of phenol by RhB$^{\bullet+}$, since high phenol concentration likely favors dye recovery via the electron delivery from phenol to RhB$^{\bullet+}$. Third, dye decolorization and phenol oxidation showed a poor kinetic correlation (Fig. 2b and its inset). It is noteworthy that RhB and MB decolorization proceeded at a comparable rate (k(RhB) = 0.0864 ± 0.0008 min^{-1} versus k(MB) = 0.0833 ± 0.0025 min^{-1} in Fig. 2b) whereas the use of RhB as a sensitizer led to 9.6-fold faster oxidation of phenol.
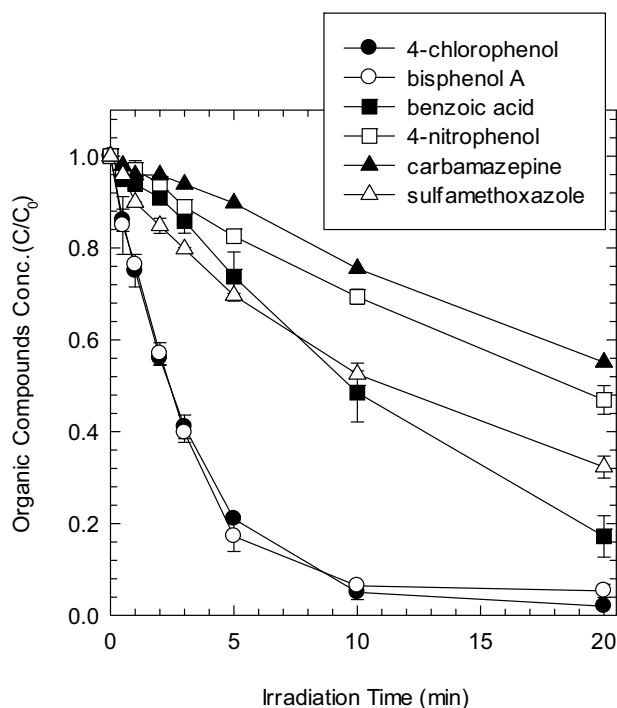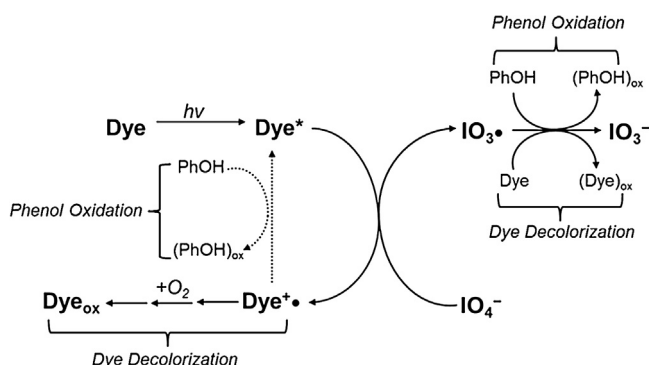
Fig. 5. Oxidative degradation of diverse organic compounds by Rhodamine B/periodate system irradiated with visible light ([Rhodamine B]$_0$ = [4-chlorophenol]$_0$ = [bisphenol A]$_0$ = [benzoic acid]$_0$ = [4-nitrophenol]$_0$ = [carbamazepine]$_0$ = [sulfamethoxazole]$_0$ = 50 μM; [periodate]$_0$ = 0.5 mM; pH$_i$ = 7.0).

Scheme 1. Proposed mechanism for the dye-sensitized activation of periodate.

This may be ascribed to the different oxidizing power of dye radical cation (e.g., RhB$^{\bullet+}$ versus MB$^{\bullet+}$).

3.6. Effects of reaction parameters

We further tested RhB decolorization and phenol decomposition under different reaction conditions and water quality parameters. First, we found that the rates of both RhB decolorization and phenol degradation increased as the RhB concentration was increased (Fig. 6a). The highest rates were observed at a RhB concentration of 50 μM, followed by a slight decline with further addition of RhB. The decrease in the rates at higher concentration is likely related to deactivation of RhB* through the self-quenching and triplet–triplet annihilation among RhB* [2,22]. When IO$_4^-$ concentration was increased up to 0.5 mM, both RhB and phenol were degraded faster (Fig. 6a). At higher IO$_4^-$ concentration (at 1.0 mM), however, phenol degradation rate decreased, while RhB degradation rate continued to increase. It is possible that excess IO$_3^\bullet$ was partly

quenched by IO$_4^-$ through the reaction IO$_4^- +$IO$_3^\bullet \rightarrow$IO$_3^- +$IO$_4^\bullet$ ($k = 2 \times 10^8$ M^{-1}s^{-1}) [12]. The counterbalancing effect of IO$_3^\bullet$ formation versus IO$_3^\bullet$ quenching by IO$_4^-$, both more effective at higher IO$_4^-$ concentration, might allow the phenol decay rate to remain fairly constant once the IO$_4^-$ concentration exceeds a certain level.

We also tested the performance of RhB/phenol/IO$_4^-$ system at varying initial pHs (Fig. 6b). The pH value did not change by more than *ca.* 0.6–0.7 unit; the final pH values of the experimental solutions initially adjusted to pH 3.0, 5.0, and 9.0 were determined as 3.14, 4.5, and 8.76, respectively. While the rate of RhB decolorization did not change in the pH range from 3.0 to 7.0, it decreased as the initial pH increased from 7.0, 9.0, up to 11.0. This change in the reactivity mirrors the change in I(VII) speciation from IO$_4^-$ to H$_3$IO$_6^{2-}$ (usually exists as a dimer form, H$_2$I$_2$O$_{10}^{4-}$) with pKa = 8.31 [18] (Fig. S20). In addition to greater repulsive interaction between H$_2$I$_2$O$_{10}^{4-}$ and negatively charged RhB (pKa = ~4.2) [23] compared to that involving IO$_4^-$, the decrease in reduction potential from 1.298 V for IO$_4^-$/IO$_3^-$ to 0.686 V for H$_3$IO$_6^{2-}$/IO$_3^-$ [24] is likely to be responsible for the observed pH dependence. The phenol degradation rate peaked at neutral pH and decreased with both increase and decrease of pH (Fig. 6b). The similar observation has been made for 4-chlorophenol decay reaching maximum rate at neutral pH when IO$_3^\bullet$ was a predominant reactant, once again confirming the proposed mechanism [11].

3.7. Photosensitized disinfection

We found that the RhB/IO$_4^-$ system can lead to a remarkably efficient visible-light-sensitized inactivation of MS2 phage (Fig. 7). We observed more than 4-log (99.99%) inactivation of MS2 phage within 30 s of visible-light irradiation using 50 μM RhB and 0.5 mM IO$_4^-$. When IO$_4^-$ concentration was lowered to 0.1 mM, we still obtained 5-log inactivation within 5 min under otherwise identical condition. No decrease in the viability of MS2 phage was observed during direct visible light photolysis of RhB (without IO$_4^-$) or IO$_4^-$ (without RhB), consistent with the observations made for phenol degradation. This result not only excludes the possibility that RhB sensitization or IO$_4^-$ activation alone induces MS2 phage inactivation (for example, through photosensitized formation of ^{1}O$_2$ from RhB), but also fortifies the involvement of IO$_3^\bullet$ in the photosensitized virus inactivation. The fact that we did not observe any significant inactivation of *E. coli* (i.e., only 1-log reduction in viability after 1 h of photo-irradiation; Fig. S21) appears to be in accordance with the selective reactivity of IO$_3^\bullet$ toward organic compounds, while there are many other factors that would contribute to the difference in inactivation kinetics between *E. coli* and MS2 phage (e.g., differences in lethal dose of IO$_3^\bullet$, difference in constituents of *E. coli* cell wall versus viral capsid), which is out of scope of this study.

3.8. Solar-Driven decolorization of dye mixtures

We suggested that this process might be suited for solar-light-driven process development, as demonstrated herein using a solar simulator for effective concomitant RhB decolorization and phenol degradation in Fig. S22. In such applications, more than one dyes can be employed to treat otherwise non-photoactive dyes such as RB5 (Fig. 2b); for example, when RhB and RB5 are used in tandem, we observed rapid degradation of RB5 through IO$_3^\bullet$-involving mechanism discovered in this study (Fig. S23a). Alternatively, a system of more than one dyes can achieve broader absorption of visible spectrum, enabling more efficient use of a wider range of incident solar spectrum. For example, while irradiation with wavelength above 650 nm caused no decomposition of RhB (with cut-off filter; data not shown), addition of MB led to decomposition of both RhB
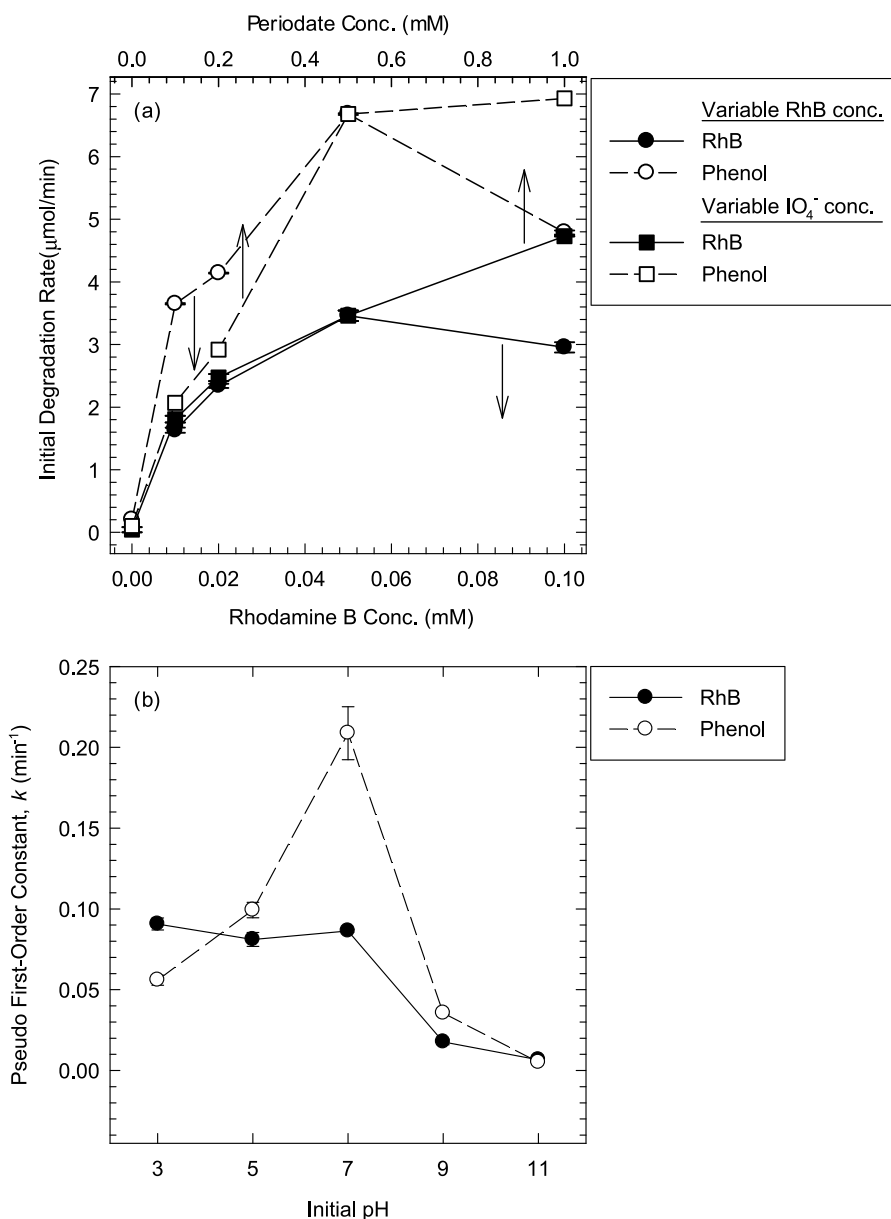
Fig. 6. (a) Kinetic rates of Rhodamine B decolorization and phenol degradation as a function of initial concentration of Rhodamine B ([Rhodamine B]$_0$ = 10, 20, 50, and 100 μM; [phenol]$_0$ = 50 μM; [periodate]$_0$ = 0.5 mM; pH$_i$ = 7.0) and initial dose of periodate ([Rhodamine B]$_0$ = [phenol]$_0$ = 50 μM; [periodate]$_0$ = 0.1, 0.2, 0.5, and 1 mM; pH$_i$ = 7.0) and (b) effect of initial pH on rates of self-sensitized Rhodamine B destruction and phenol decomposition ([Rhodamine B]$_0$ = [phenol]$_0$ = 50 μM; [periodate]$_0$ = 0.5 mM; pH$_i$ = 3.0, 5.0, 7.0, 9.0, and 11.0).

and MB through MB sensitization and subsequent IO$_3^\bullet$ production (Fig. S23b).

4. Conclusion

In an effort to test a hypothetic role of IO$_4^-$ as a substitute for TiO$_2$ in the self-sensitized dye decolorization, this study elucidates and introduces a new photochemical IO$_4^-$ activation mechanism in which visible-light-sensitized electron transfer from dye to IO$_4^-$ and accompanying reactive radical formation achieve the degradation of dye as well as other organics co-present in water. The mechanism investigated herein presents an untapped opportunity to utilize photon energy in visible spectrum to initiate a sequence of redox reactions that can be instrumental in environmental remediation scenarios; for example, electron transfer from the visible light responsive organics (e.g., dyes and NOMs) to metal ions (e.g., Cr^{6+},

Ag$^+$) or oxyanions (e.g., HSO$_5^-$), resulting in heavy metal detoxification, noble metal recovery, or production of oxidizing radicals.

The selective reactivity of IO$_3^\bullet$ and effectiveness at neutral pH indicate potential application of the proposed reaction scheme in treatment of complex water matrix (e.g., textile wastewater). The use of an unconventional oxyanion, IO$_4^-$, might discourage application in drinking water treatment; for water reclamation scenarios, subsequent cost-effective treatment technologies such as adsorption and ion-exchange are well-established for IO$_3^-$ removal [25] and electrochemical oxidation of IO$_3^-$ for regeneration of IO$_4^-$ [26]. Note that iodide (I$^-$) does not form during IO$_4^-$ activation and IO$_3^-$ is the most desirable end product among iodine species (e.g., I$_2$, IO$_4^-$) due to relatively low toxicity [27] and minimal iodinated byproduct formation potential [28]. The proposed photosensitization process to initiate the concurrent degradation of dyes and organics appears operable under natural sunlight irradiation based on the performance under irradiation of visible light ($\lambda > 400$ nm)
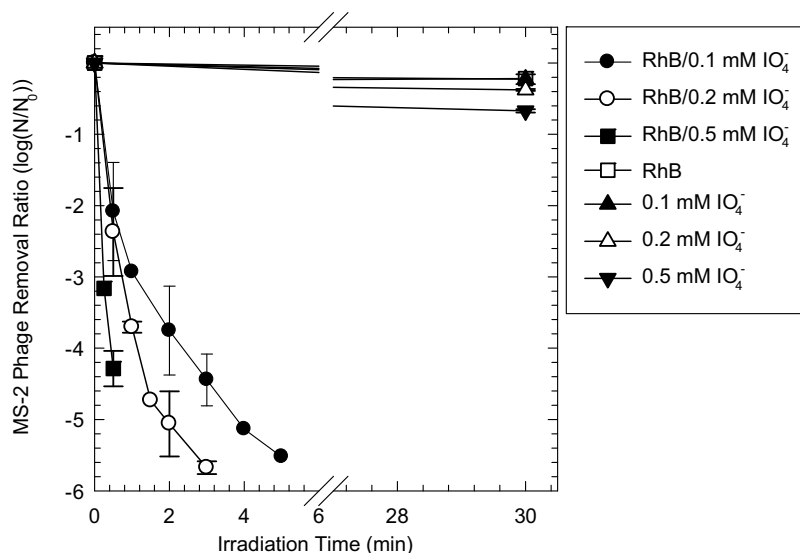
Fig. 7. Inactivation of MS2 phage by the Rhodamine B/periodate system under visible light irradiation ([MS 2 phage]$_0$ = 10^7 PFU/mL; [Rhodamine B]$_0$ = 50 μM; [periodate]$_0$ = 0.1, 0.2, and 0.5 mM; [phosphate buffer]$_0$ = 1 mM; pH$_i$ = 7.0).

and artificial sunlight. In particular, practical application for treatment of dye mixtures (mimicking the composition of real textile wastewater) can bring technical benefits to the solar-driven decoloration involving IO_4^-: performance independent of the type of dye sensitizer and photoresponse extended into longer wavelength region.

Appendix A. Supplementary data

Supplementary data associated with this article can be found, in the online version, at http://dx.doi.org/10.1016/j.apcatb.2016.10.029.

References

[1] J.R. Bunting, Photochem. Photobiol. 55 (1992) 81–87.
[2] M.C. DeRosa, R.J. Crutchley, Coord. Chem. Rev. 233 (2002) 351–371.
[3] N.A. Garcia, J. Photochem. Photobiol. B 22 (1994) 185–196.
[4] J. Lenard, R. Vanderoef, Photochem. Photobiol. 58 (1993) 527–531.
[5] C.C. Chen, W.H. Ma, J.C. Zhao, Chem. Soc. Rev. 39 (2010) 4206–4219.
[6] T.X. Wu, G.M. Liu, J.C. Zhao, H. Hidaka, N. Serpone, J. Phys. Chem. B 102 (1998) 5845–5851.
[7] U. Bach, D. Lupo, P. Comte, J.E. Moser, F. Weissortel, J. Salbeck, H. Spreitzer, M. Gratzel, Nature 395 (1998) 583–585.
[8] G.M. Liu, T.X. Wu, J.C. Zhao, H. Hidaka, N. Serpone, Environ. Sci. Technol. 33 (1999) 2081–2087.
[9] H. Kyung, J. Lee, W.Y. Choi, Environ. Sci. Technol. 39 (2005) 2376–2382.
[10] H. Kim, H.Y. Yoo, S. Hong, S. Lee, S. Lee, B.S. Park, H. Park, C. Lee, J. Lee, Appl. Catal. B. Environ. 162 (2015) 515–523.
[11] H. Lee, H.Y. Yoo, J. Choi, I.H. Nam, S. Lee, S. Lee, J.H. Kim, C. Lee, J. Lee, Environ. Sci. Technol. 48 (2014) 8086–8093.
[12] L.H. Chia, X.M. Tang, L.K. Weavers, Environ. Sci. Technol. 38 (2004) 6875–6880.
[13] C. Lee, J. Yoon, J. Photochem. Photobiol. A 165 (2004) 35–41.
[14] F.L. Zhang, J.C. Zhao, T. Shen, H. Hidaka, E. Pelizzetti, N. Serpone, Appl. Catal. Environ. 15 (1998) 147–156.
[15] M. Cho, H.M. Chung, W.Y. Choi, J.Y. Yoon, Appl. Environ. Microbiol. 71 (2005) 270–275.
[16] A.J. Bard, R. Parsons, J. Jordan, Standard Potentials in Aqueous Solution, CRC Press, New York, 1985.
[17] E.A. Betterton, M.R. Hoffmann, Environ. Sci. Technol. 24 (1990) 1819–1824.
[18] J.-L. Burgot, Ionic Equilibria in Analytical Chemistry, Springer, 2012, pp. 347–367.
[19] P.C. Beaumont, D.G. Johnson, P.J. Parsons, J. Photochem. Photobiol. A 107 (1997) 175–183.
[20] U. Stafford, K.A. Gray, P.V. Kamat, J. Phys. Chem. 98 (1994) 6343–6351.
[21] R.I. Samoilova, A.R. Crofts, S.A. Dikanov, J. Phys. Chem. A 115 (2011) 11589–11593.
[22] A.K. Chibisov, J. Photochem. 6 (1977) 199–214.
[23] N.S. Maurya, A.K. Mittal, P. Cornel, E. Rother, Bioresour. Technol. 97 (2006) 512–521.
[24] A. Mills, D. Hazafy, S. Elouali, C. O'Rourke, J. Mater. Chem. A 4 (2016) 2863–2872.
[25] K.H. Goh, T.T. Lim, Z. Dong, Water Res. 42 (2008) 1343–1368.
[26] M. Okochi, H. Yokokawa, T.K. Lim, T. Taguchi, H. Takahashi, H. Yokouchi, T. Kaiho, A. Sakuma, T. Matsunaga, Appl. Environ. Microbiol. 71 (2005) 6410–6413.
[27] X. Hou, Comprehensive Handbook of Iodine: Nutritional, Biochemical, Pathological and Therapeutic Aspects, Academic Press, 2009, pp. 139–150.
[28] S. Allard, C.E. Nottle, A. Chan, C. Joll, U. von Gunten, Water Res. 47 (2013) 1953–1960.